



HAL
open science

Spatial Markov processes for modeling Lagrangian particle dynamics in heterogeneous porous media

Tanguy Le Borgne, Marco Dentz, Jesus Carrera

► **To cite this version:**

Tanguy Le Borgne, Marco Dentz, Jesus Carrera. Spatial Markov processes for modeling Lagrangian particle dynamics in heterogeneous porous media. *Physical Review E : Statistical, Nonlinear, and Soft Matter Physics*, 2008, 78, pp.026308. 10.1103/PhysRevE.78.026308 . insu-00372038

HAL Id: insu-00372038

<https://insu.hal.science/insu-00372038>

Submitted on 8 Mar 2022

HAL is a multi-disciplinary open access archive for the deposit and dissemination of scientific research documents, whether they are published or not. The documents may come from teaching and research institutions in France or abroad, or from public or private research centers.

L'archive ouverte pluridisciplinaire **HAL**, est destinée au dépôt et à la diffusion de documents scientifiques de niveau recherche, publiés ou non, émanant des établissements d'enseignement et de recherche français ou étrangers, des laboratoires publics ou privés.

Spatial Markov processes for modeling Lagrangian particle dynamics in heterogeneous porous media

Tanguy Le Borgne*

Géosciences Rennes, UMR 6118, CNRS, Université de Rennes 1, Rennes, France

Marco Dentz

Department of Geotechnical Engineering and Geosciences, Technical University of Catalonia (UPC), Barcelona, Spain

Jesus Carrera

Institute of Environmental Analysis and Water Studies (IDAEA), CSIC, Barcelona, Spain

(Received 28 April 2008; published 26 August 2008)

We investigate the representation of Lagrangian velocities in heterogeneous porous media as Markov processes. We use numerical simulations to show that classical descriptions of particle velocities using Markov processes in time fail because low velocities are much more strongly correlated in time than high velocities. We demonstrate that Lagrangian velocities describe a Markov process at fixed distances along the particle trajectories (i.e., a spatial Markov process). This remarkable property has significant implications for modeling effective transport in heterogeneous velocity fields: (i) the spatial Lagrangian velocity transition densities are sufficient to fully characterize these complex velocity field organizations, (ii) classical effective transport descriptions that rely on Markov processes in time for the particle velocities are not suited for describing transport in heterogeneous porous media, and (iii) an alternative effective transport description derives from the Markovian nature of the spatial velocity transitions. It expresses particle movements as a random walk in space time characterized by a correlated random temporal increment and thus generalizes the continuous time random walk model to transport in correlated velocity fields.

DOI: [10.1103/PhysRevE.78.026308](https://doi.org/10.1103/PhysRevE.78.026308)

PACS number(s): 47.56.+r, 05.40.Fb, 05.10.Gg, 05.60.-k

I. INTRODUCTION

The transport of chemicals in groundwater, the ocean, or the atmosphere is controlled by the multiscale organization of natural flows. Natural flow fields generally have a complex organization characterized by heterogeneous structures at different scales [1–4]. Transport in such velocity fields displays non-Fickian characteristics such as strong tailing of first arrival times and non-Gaussian spatial distributions (e.g., [5]). Accounting for these properties is particularly critical for the prediction of contaminant transport in the subsurface, which is the focus of the present study. A number of approaches such as continuous time random walk (CTRW) theory and fractional Fokker-Planck equations describe anomalous transport [6–11]. For transport in shear flows the role of the flow organization for effective transport can be quantified exactly [12]. For many natural flow scenarios cases, however, and in particular for transport in groundwater flows, the role of the local flow organization on effective transport is not understood quantitatively [13,14] which limits our predictive capabilities.

Let us consider the one-dimensional space-time random walk model,

$$x^{(n+1)} = x^{(n)} + \xi^{(n)}, \quad t^{(n+1)} = t^{(n)} + \tau^{(n)}, \quad (1)$$

where both the spatial and temporal increments $\xi^{(n)}$ and $\tau^{(n)}$ are random. Equation (1) describes a continuous time random walk (CTRW) (e.g., [15]). The particle velocity at step

n is given by the kinematic relationship $v^{(n)} = \xi^{(n)} / \tau^{(n)}$. Note that it may include advection and diffusion processes. The space-time positions of a particle after n steps are denoted by $(x^{(n)}, t^{(n)})$. Non-Fickian transport can be modeled in this framework by choosing the spatio-temporal increments from distributions whose widths are of the order of or larger than the observation scales. Fickian behavior is obtained if both the widths of the distributions of the spatial and temporal increments are small compared to the observation lengths and times.

The application of effective random walk models to the description of effective transport in heterogeneous velocity fields is often based on the postulation of a joint distribution of the spatial and temporal increments and the subsequent fit of the model to some dispersion measurements (such as the evolution of the spatial moments of the solute cloud or breakthrough curves). However, the relationship between the flow field organization and the distribution of spatial and temporal increments is unknown in general. In particular, in many effective random walk descriptions velocity correlation properties, which carry information on the velocity field organization, cannot be included easily [16].

Here, we derive a joint distribution of spatial and temporal increments from the Lagrangian velocity statistics and correlation properties instead of postulating it. The Lagrangian statistics are obtained from numerical simulations of flow and transport in highly heterogeneous porous media. Lagrangian flow characteristics play an important role for the qualitative and quantitative understanding of non-Fickian transport in heterogeneous flow fields [13]. Specifically, strong correlations have been identified as a cause for non-

*tanguy.le-borgne@univ-rennes1.fr

Fickian transport patterns (e.g., [7]). A different source for non-Fickian transport is broad disorder distributions (e.g., [17]). Long disorder correlations on one hand and broad heterogeneity distributions on the other hand are possible causes for anomalous transport patterns with different impact on the effective transport behavior. Our ultimate objective is to define an effective transport model that is consistent with the velocity fields organization and that is fully characterized by the Lagrangian velocity statistics.

In this paper we analyze the Lagrangian flow characteristics with the aim to obtain a simple formulation for effective particle dynamics as a Markovian model. To this end we set up a numerical random walk model for transport in a heterogeneous Darcy flow field, project the transport process on the direction of the mean flow, and analyze the Lagrangian velocity statistics along the projected particle trajectories. The latter defines a $d=1$ dimensional stochastic process that turns out to be a Markov chain for constant spatial increments, i.e., the velocity at a given position along the trajectory depends only on the velocity value at the previous positions. The transition time between two particle positions along the trajectory is given by the (constant) transition length and (projected) flow velocity. The latter defines a correlated continuous time random walk.

II. PRELIMINARY REMARKS

Advective-diffusive solute transport is described by mass balance, i.e., the temporal change of the solute concentration $c(\mathbf{x}, t)$ is balanced by the divergence of the advective and diffusive solute fluxes. This mass balance is expressed by the Fokker-Planck equation

$$\Phi \frac{\partial c(\mathbf{x}, t)}{\partial t} + \mathbf{q}(\mathbf{x}) \cdot \nabla c(\mathbf{x}, t) - D \nabla^2 c(\mathbf{x}, t) = 0, \quad (2)$$

where D is the (constant) diffusion coefficient, and the porosity Φ is set equal to one. Note that for simplicity here we consider isotropic and constant diffusion. The Eulerian velocity field $\mathbf{q}(\mathbf{x})$ is given as the divergence-free solution of the Darcy equation [18]

$$\mathbf{q}(\mathbf{x}) = -K(\mathbf{x}) \nabla h(\mathbf{x}), \quad (3)$$

where $h(\mathbf{x})$ is the hydraulic head. The hydraulic conductivity $K(\mathbf{x})$ reflects the spatial medium heterogeneity.

The Fokker-Planck equation (2) is exactly equivalent to the Langevin equation (e.g., [19])

$$\frac{d\mathbf{x}(t)}{dt} = \mathbf{q}[\mathbf{x}(t)] + \boldsymbol{\xi}(t), \quad (4)$$

which describes the trajectory $\mathbf{x}(t)$ of a solute particle in time. Diffusion is simulated by the Gaussian white noise $\boldsymbol{\xi}(t)$, which is characterized by zero mean and the variance $\langle \xi_i(t) \xi_j(t') \rangle = D \delta_{ij} \delta(t-t')$; the angular brackets denote the noise average. The particle distribution $c(\mathbf{x}, t)$ is given in terms of the particles trajectories as

$$c(\mathbf{x}, t) = \langle \delta[\mathbf{x} - \mathbf{x}(t)] \rangle. \quad (5)$$

In the following, we focus on transport in a $d=2$ dimensional heterogeneous medium. The position vector $\mathbf{x}=(x, y)^T$.

Equation (4) describes transport in a single realization of the heterogeneous medium. In most practical cases, however, a detailed medium description is not available and also not desirable. What one seeks is an effective transport description that incorporates the impact of heterogeneity on effective transport in a systematic manner. The latter can be achieved by upscaling. The aim here is to describe the effective transport behavior by using a statistical heterogeneity characterization. To this end, the salient (statistical) features of heterogeneity that determine effective transport need to be identified and quantified. Stochastic modeling provides a systematic way to do so.

In a stochastic approach, the spatially variable hydraulic conductivity field $K(\mathbf{x})$ represents a typical realization of a spatial stochastic process. The latter is usually characterized by the (functional) distribution of the log hydraulic conductivity function $f(\mathbf{x}) = \ln[K(\mathbf{x})]$, $\mathcal{P}\{f(\mathbf{x})\}$. We consider here stationary random fields, i.e., fields for which $\mathcal{P}\{f(\mathbf{x}+\mathbf{L})\} = \mathcal{P}\{f(\mathbf{x})\}$, with \mathbf{L} a constant translation. In the following, the mean value $\overline{f(\mathbf{x})}$ is set to zero. The two-point correlation function of $f(\mathbf{x})$ then is given by

$$\overline{f(\mathbf{x})f(\mathbf{x}')} = C_f(\mathbf{x} - \mathbf{x}'). \quad (6)$$

The overline denotes the ensemble average over all realization of the spatial random process $\{f(\mathbf{x})\}$. The correlation function $C_f(\mathbf{x})$ here is given by the Gaussian shaped function

$$C_f(\mathbf{x}) = \sigma_f^2 \exp\left(-\frac{\mathbf{x}^2}{\lambda}\right), \quad (7)$$

where λ is the correlation length of the log-hydraulic conductivity field and σ_f^2 its variance, $\sigma_f^2 = \overline{f(\mathbf{x})^2}$. The random velocity field is stationary as a consequence of the stationarity of $f(\mathbf{x})$ and can be decomposed into its (constant) mean value and fluctuations about it,

$$\mathbf{q}(\mathbf{x}) = \bar{\mathbf{q}} + \mathbf{q}'(\mathbf{x}). \quad (8)$$

The (Eulerian) correlation of $\mathbf{q}(\mathbf{x})$ is given by

$$\overline{q'_i(\mathbf{x})q'_j(\mathbf{x}')} \equiv C_{ij}^E(\mathbf{x} - \mathbf{x}'). \quad (9)$$

Without loss of generality, the one-direction of the coordinate system is aligned here with the mean flow direction so that $\bar{\mathbf{q}} = \mathbf{e}_1 \bar{q}$, where \mathbf{e}_1 is the unit vector in one-direction.

Note that the particle movement described by Eq. (4) depends on two stochastic processes, the spatially varying random velocity field, and the temporal noise term. The aim is to represent effective transport as a random walk that is completely characterized by the Lagrangian velocity statistics, i.e., by the statistics of $\mathbf{q}[\mathbf{x}(t)]$. The Lagrangian velocity correlation is defined by

$$C_{ij}^L(t-t') = \overline{q'_i[\mathbf{x}(t)]q'_j[\mathbf{x}(t')]}. \quad (10)$$

The particle velocity is given by

$$\mathbf{v}(t) = \bar{q}\mathbf{e}_1 + \mathbf{q}'[\mathbf{x}(t)] + \boldsymbol{\xi}(t). \quad (11)$$

The correlation of the velocity fluctuations in the Ito interpretation then reads as

$$\overline{v'_i(t)v'_j(t')} = C_{ij}^L(t-t') + 2D\delta_{ij}\delta(t-t'), \quad (12)$$

Here we study effective random walk descriptions of the transport problem (4) as given by Eq. (1). Let us consider the discretized version of Eq. (4):

$$\mathbf{x}^{(n+1)} = \mathbf{x}^{(n)} + \mathbf{q}(\mathbf{x}^{(n)})\Delta t + \sqrt{2D\Delta t}\boldsymbol{\eta}^{(n)}, \quad (13)$$

$$t^{(n+1)} = t^{(n)} + \Delta t, \quad (14)$$

where $\boldsymbol{\eta}^{(n)}$ is a Gaussian random variable with zero mean and unit variance. In an effective description, we want to substitute the nonlinear noise term $\mathbf{q}[\mathbf{x}(t)]$ by a noise term that does not depend on the (effective) particle trajectory but only on the number of steps of the effective random walk. Projection of the particle motion on the direction of mean flow yields the equation of motion

$$x^{(n+1)} = x^{(n)} + q_1(\mathbf{x}^{(n)})\Delta t + \sqrt{2D\Delta t}\eta^{(n)}, \quad (15)$$

$$t^{(n+1)} = t^{(n)} + \Delta t,$$

To represent transport in an ensemble sense, the statistics of $q_1[\mathbf{x}(t)]$, which depends on the particle trajectory, need to be explored. This can be done in two different ways. The first way is to define an equivalent description of Eq. (15) by

$$x^{(n+1)} = x^{(n)} + v_t^{(n)}\Delta t, \quad t^{(n+1)} = t^{(n)} + \Delta t. \quad (16)$$

Here, $\{v_t^{(n)}\}_{n=0}^{\infty}$ is a stochastic process that is defined by the ensemble statistics of the Lagrangian velocity field along the projected particle trajectory at equidistant times. However, the process $\{v_t^{(n)}\}_{n=0}^{\infty}$ does not need to be Markovian, and in general is not. For transport in Gaussian random shear flow the description (16) turns out to be an equivalent effective random walk model [12] with $\{v_t^{(n)}\}$ a correlated Gaussian noise. For lognormally distributed hydraulic conductivity fields, Fiori and Dagan [20] established an approximate effective random walk description, whose (correlated) noise is characterized by the first-order approximation of the Lagrangian correlation function $C_{ij}^L(t)$ in the variance of the log-hydraulic conductivity field.

If it is possible to define a (finite) characteristic transition length over which the velocity field is approximately constant we can define an alternative effective random walk model by

$$x^{(n+1)} = x^{(n)} + \Delta x, \quad t^{(n+1)} = t^{(n)} + \frac{\Delta x}{v_s}. \quad (17)$$

For the heterogeneity scenarios under consideration, the characteristic length is given by the correlation scale λ of the log-hydraulic conductivity field. In fact, the correlation scale of the (Eulerian) flow velocity is in general larger than λ so that a choice of Δx of the order of or smaller than λ should be sufficient, i.e., $\Delta x \leq \lambda$. Here, the stochastic process $\{v_s^{(n)}\}_{n=0}^{\infty}$ is defined by the Lagrangian ensemble statistics along the projected particle trajectory at equidistant spatial locations. In the following, we focus on the analysis and characterization of the processes $\{v_t^{(n)}\}_{n=0}^{\infty}$ and $\{v_s^{(n)}\}_{n=0}^{\infty}$.

III. NUMERICAL SETUP AND TRANSPORT BEHAVIOR

Here we consider different hydraulic conductivity fields that have the same point distributions but different spatial

structures. Figure 1 illustrates three types of velocity fields and the corresponding flow fields. We use particle tracking simulations in $d=2$ dimensional heterogeneous hydraulic conductivity fields in order to compute the Lagrangian velocity and investigate its transition properties in space and time.

We solve flow and transport in two-dimensional heterogeneous hydraulic conductivity fields. At the boundaries we impose permeameterlike conditions: no flux across the lateral boundaries and constant head at the upstream and downstream boundaries. The flow equation is solved numerically with a finite difference scheme using a grid of 512×512 elements. Once the flow field is obtained, solute transport is simulated by random walk particle tracking (e.g., [21]), i.e., numerical iteration of Eq. (14). Flow velocities are interpolated using a bilinear interpolation scheme (e.g., [22]).

We consider here advection-dominated transport scenarios. The relative importance of advective and diffusive transport mechanisms is measured by the Peclet number. The latter is defined in terms of the geometric mean of the hydraulic conductivity field \bar{K} , the pixel size d , and the diffusion coefficient D as $Pe = \frac{d\bar{K}}{D}$. For large Pe , transport is advection-dominated and vice versa. The mean hydraulic gradient is set to one. The Peclet number is set to $Pe=10^2$, which is a typical value for solute transport in heterogeneous geological formations. The influence of the Peclet number on the velocity correlation properties will be investigated in a further study. Solute particles are tracked within 100 hydraulic conductivity field realizations. The particles are injected along a centered vertical line of 200 elements length located in a distance of 64 elements from the upstream boundary. They are injected proportionally to the local flow. The numerical solution of the flow problem and the implementation of the particle tracking method are described in more details in [13].

We consider three types of hydraulic conductivity fields: (i) multilognormal fields, (ii) connected multilognormal fields, and (iii) multilognormal stratified fields. For the multilognormal hydraulic conductivity field [Fig. 1(a)], the variance is and the correlation length is $\lambda=8$ (in units of elements), i.e., the medium size is $64 \times 64 \lambda$. For the generation of the lognormal hydraulic conductivity fields with connected high hydraulic conductivity zones [Fig. 1(b)], we use the method described in Refs. [23,24]. The resulting hydraulic conductivity has the same point value distribution and approximately the same two-point correlation as the multilognormal hydraulic conductivity field described above. For the stratified hydraulic conductivity field [Fig. 1(c)], a hydraulic conductivity is randomly assigned to each (one element wide) horizontal stratum. Thus, here the correlation structure is highly anisotropic as the longitudinal correlation length is infinite, the transverse correlation length is of the order of one.

The three hydraulic conductivity fields have identical point distributions of hydraulic conductivity values. They are different with respect to their respective spatial organization. The degree of organization of the hydraulic conductivity fields increases from top to bottom in Fig. 1. The calculated point velocity distributions are given in Fig. 2. They are

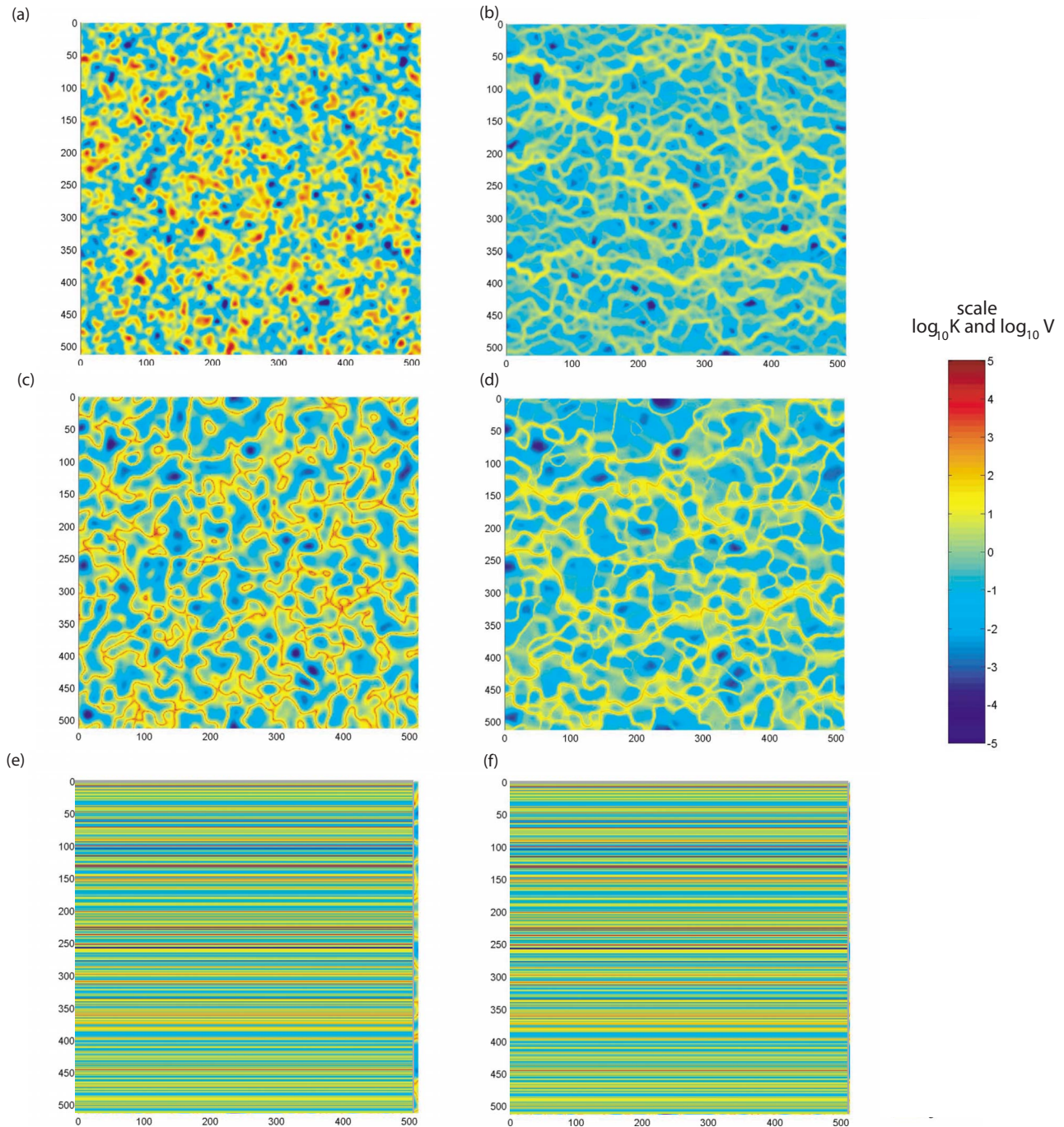


FIG. 1. (Color online) Hydraulic conductivity K and modulus of velocity v . (a) Multilognormal hydraulic conductivity field ($\sigma_f^2=9$, $\lambda=8$, size 512×512 elements), (b) corresponding velocity field, (c) connected hydraulic conductivity field, (d) corresponding velocity field, (e) stratified hydraulic conductivity field, and (f) corresponding velocity field. These three fields have the same point distribution of hydraulic conductivity values.

highly heterogeneous with a range of about eight orders of magnitude. The characteristic distance of the fields of the first and second type is the correlation length λ , which, together with the geometric mean of the hydraulic conductivity field \bar{K} defines the characteristic advection time scale $\tau = \lambda / \bar{K}$. Note, however, that the velocity field organization implies a range of (Lagrangian) velocity correlation lengths and times [13]. The high heterogeneity of the hydraulic conductivity field leads to connected high velocity zones and

strong focusing of the streamlines [Figs. 1(a) and 1(b)]. In the following, we propose a method to quantify the Lagrangian correlation lengths and times.

First, however, let us illustrate the effect of connectivity on solute dispersion. To this end, we first display arrival time distributions at a distance of 100 elements from the inlet (Fig. 3). The first arrival time decreases and the late time tailing increases with increasing connectivity. Notice that the late time tails are due to low particle velocities. However,

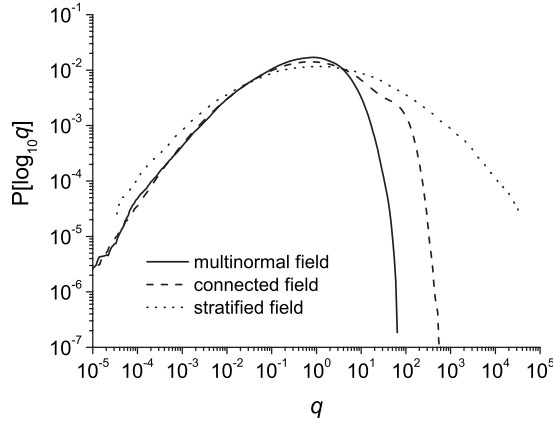


FIG. 2. Distributions of the decimal logarithm of absolute value of the Eulerian velocity.

even though all three hydraulic conductivity fields have similar distributions of the low velocity values (Fig. 2) they display different tails of the first arrival time distribution. It needs to be concluded that the breakthrough curve tailing is not entirely controlled by the point velocity distribution. It is also controlled by the velocity correlation properties. Thus the hydraulic conductivity organization and its correlation properties have a strong impact on the non-Fickian transport properties and the relevant effective equation.

IV. LAGRANGIAN VELOCITY STATISTICS

For the stratified case, the Lagrangian velocity statistics are known (e.g., [7,12,25]). The process is stationary and characterized by a power-law correlation function. The latter is due to the fact that velocity transitions here are equivalent to particle transitions between strata by lateral diffusion. Thus the probability to return to a given stratum, i.e., to a certain velocity value decreases with travel time as $t^{-1/2}$ (e.g., [7,12]). The return probability and thus the Lagrangian correlation is the same for all initial velocities. For the lognormal hydraulic conductivity fields [Figs. 1(a) and 1(b)] this is different. As shown in the following, here the Lagrangian velocity correlation at equidistant times, i.e., for the process $\{v_t^{(n)}\}_{n=0}^{\infty}$ depends on the initial velocity $v_t^{(0)}$. Specifically, low velocities turn out to be more strongly correlated than high velocities.

In the following, we propose a methodology to characterize and analyze these processes in terms of transition probabilities for the random processes $\{v_t^{(n)}\}_{n=0}^{\infty}$ and $\{v_s^{(n)}\}_{n=0}^{\infty}$, respectively. Recall that the former is defined by the Lagrangian velocity statistics at equidistant times along the particle trajectories while the latter is defined by the Lagrangian statistics at equidistant positions along the trajectories.

A. Definition of velocity classes

We discretize the particle velocity into $n-1$ classes $\{C_i\}_{i=1 \leq i \leq n-1}$ of equal probability of occurrence. We define $y = P(v)$ as the score corresponding to the velocity v where $P(v)$ is the cumulative Lagrangian velocity distribution. We

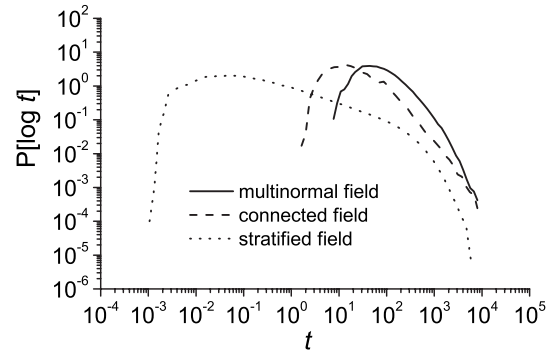


FIG. 3. Breakthrough curves for each of the hydraulic conductivity fields, at a distance equal to 100 elements from the particle inlet. The breakthrough curves are averaged over 100 hydraulic conductivity field realizations.

discretize the y domain, which is bounded between 0 and 1, into $n-1$ classes of equal width $1/(n-1)$, defined by their boundaries y_i . The smallest velocity corresponds to $y_1=0$ and the largest velocity to $y_n=1$. In this study, we use 49 classes ($n=50$). For a given velocity v the corresponding class C_i is determined as follows: $v \in C_i$ if $y_i \leq P(v) < y_{i+1}$.

B. Velocity transitions

We define $t(x)$ as the first passage time of a particle at the longitudinal location x . For a particle at longitudinal distance x from the inlet, at time $t(x)$, we define the longitudinal Lagrangian velocity as

$$v_L = \frac{x_{n+1} - x}{t(x_{n+1}) - t(x)}, \quad (18)$$

where x_{n+1} is the downstream coordinate of the pixel in which the particle is moving. Thus the Lagrangian velocity is defined as the average velocity across an incremental length $x_{n+1}-x$. It includes both advective and diffusive motions. The practical advantage of this definition is that all velocities v_L are positive. Particle velocities along particle trajectories are quantified at given times $v_t(t)$ and at given longitudinal locations $v_s(x)$.

We consider velocity transitions along the particle trajectory (i) depending on the travel time and (ii) depending on the travel distance along the trajectory projected on the mean flow direction. Thus we define (i) the probability for a particle to make a transition from velocity v' at travel time t' to the velocity v at travel time t ,

$$r_t(v, t | v', t') = \langle \delta[v - v_t(t)] \rangle |_{v_t(t')=v'} \quad (19)$$

and (ii) the probability for a particle to make a transition from velocity v' at travel distance x' to the velocity v at travel time x ,

$$r_s(v, x | v', x') = \langle \delta[v - v_s(x)] \rangle |_{v_s(x')=v'}. \quad (20)$$

Note that the transition distributions are stationary in time, i.e., $r_t(v, t | v', t') = r_t(x, t-t' | x')$ and space, $r_s(v, x | v', x') = r_s(v, x-x' | v')$, respectively, because the log-conductivity $f(\mathbf{x})$ is modeled as a stationary random field.

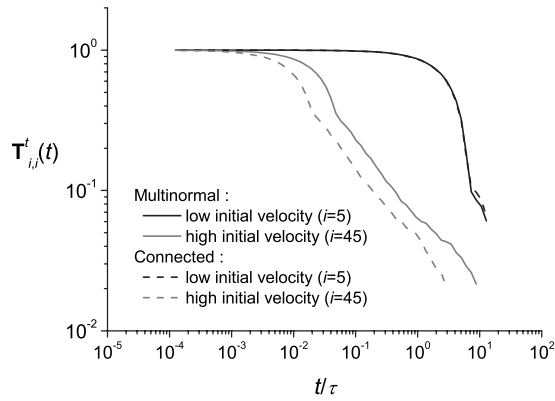


FIG. 4. Probability of returning to the initial velocity as a function of travel time for a low initial velocity $T_{5,5}^t(t)$ (black lines) and for a high initial velocity $T_{45,45}^t(t)$ (gray lines), for the multilognormal and connected (dotted lines) hydraulic conductivity fields.

Here, velocities are binned into velocity classes of equal probability. Thus in the following we consider transition probabilities between velocity classes. The probability to make a transition from a velocity $v' \in C_j$ at time $t'=0$ to a velocity $v \in C_i$ at time t is given by

$$T_{ij}^t(t) = \int_{v_i}^{v_{i+1}} dv \int_{v_j}^{v_{j+1}} dv' r_i(v, t | v', 0), \quad (21)$$

while the probability to make a transition from a velocity $v' \in C_j$ at location $x'=0$ to a velocity $v \in C_i$ at location x is given by

$$T_{ij}^s(x) = \int_{v_i}^{v_{i+1}} dv \int_{v_j}^{v_{j+1}} dv' r_s(v, x | v', 0), \quad (22)$$

$T^t(t)$ and $T^s(x)$ are the temporal and spatial velocity transition matrices for the temporal increment t and the spatial increment x , respectively.

1. Probability of returning to the initial velocity

First, we study the diagonal elements of the transition matrices (21) and (22), $T_{ii}^t(t)$ and $T_{ii}^s(x)$, respectively. The diagonal elements describe the probability for a particle to return to the same velocity as the initial velocity after a certain travel time or travel distance. Figures 4 and 5 display $T_{ii}^t(t)$ and $T_{ii}^s(x)$ for a low initial velocity class C_5 and a high initial velocity class C_{45} . An expected, yet remarkable result is that the return probability in time is much higher for low velocities than for high velocities (Fig. 4), which implies that the return probabilities have different temporal range. This is different for the stratified case, for which the return probability is independent of the initial velocity. This effect can be explained by the fact that particles take a much longer time to leave the (spatially confined) low velocity regions than the high velocity regions by advection, see Fig. 1. This type of dependence on the initial velocities is usually not accounted for in correlated random walk models as presented in, e.g., [20].

For the return probability as a function of travel distance $T_{ii}^s(x)$, we find very different results. The return probabilities

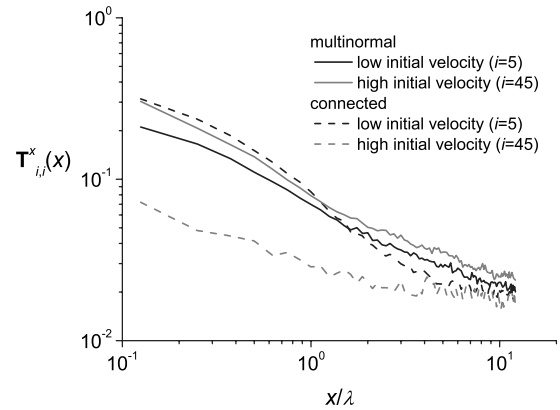


FIG. 5. Probability of returning to the initial velocity as a function of travel distance for the two extreme velocity classes, $T_{5,5}^s(x)$ and $T_{45,45}^s(x)$, for the multilognormal and connected hydraulic conductivity fields.

for the high and low velocities have a narrow spatial range (Fig. 5). Thus the Lagrangian velocity field for the multilognormal hydraulic conductivity field is characterized by a broad range of correlation times [as quantified by $T_{ii}^t(t)$] but by a relatively narrow range of correlation distances [as quantified by $T_{ii}^s(x)$].

For the connected field we find similar results as for the multilognormal field (Figs. 4 and 5), except that the difference between the return probabilities for high and low initial velocities increases. This can be explained by the topology of the velocity fields (Fig. 1). High velocity paths tend to be narrower in the connected fields, so that diffusion can take particles to low velocity regions faster than in multilognormal fields.

2. Transition probability matrix

In this section, we compute the full velocity transition matrix, which describes the probability for a particle starting in a given velocity class to make a transition to another velocity class. As a consequence of the stationarity of the Lagrangian velocity distribution $P(v)$, the transition matrix at any given travel time or distance has the property

$$\sum_{i=1}^n T_{ij}^t(t) = \sum_{j=1}^n T_{ij}^t(t) = \sum_{i=1}^n T_{ij}^s(x) = \sum_{j=1}^n T_{ij}^s(x) = 1. \quad (23)$$

Figures 6 and 7 display the transition matrices for the different hydraulic conductivity fields at travel time $t=\tau/2$ and travel distance $x=\lambda/2$. The transition matrices in time for the multilognormal and connected fields are found to be symmetric with respect to the principal diagonal but very asymmetric with respect to the secondary diagonal (Fig. 6). This reflects the fact that the temporal correlation properties depend strongly on the initial velocity. Particles that start at high initial velocities can, within the same time interval, jump to other velocities whereas particles that start at low initial velocities can only jump to velocities that are relatively close to the initial velocity.

The transition matrix $T_{ij}^s(x)$ in space is found to be nearly symmetric for the multilognormal hydraulic conductivity

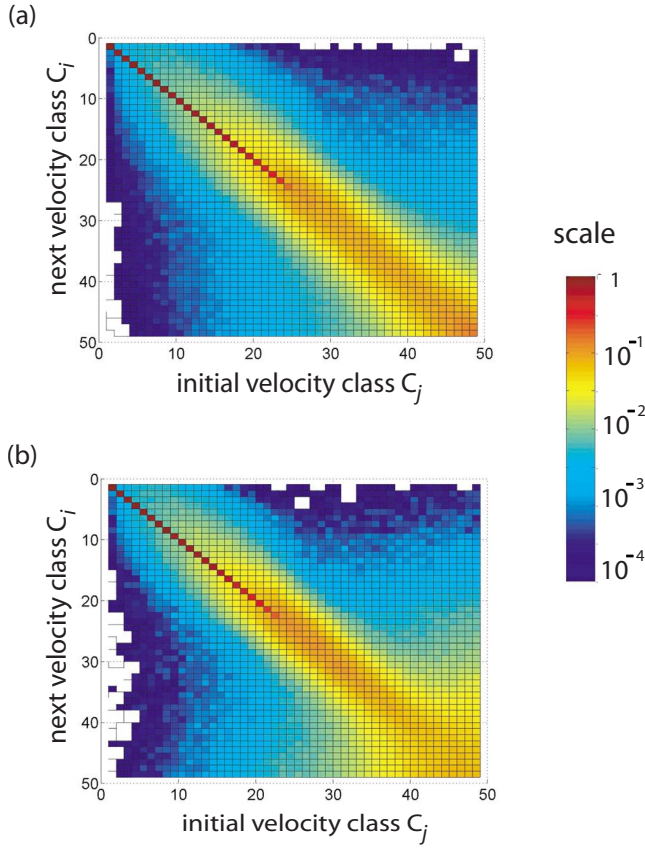


FIG. 6. (Color online) Transition matrix in time $\mathbf{T}^t(\tau/2)$ for the multilognormal field and the connected field.

field [Fig. 7(a)]. This is consistent with the fact that the return probabilities for high and low initial velocities are nearly identical (Fig. 5). The transition matrix $T_{ij}^s(x)$ for the connected hydraulic conductivity field is slightly asymmetric with a higher return probability for the low velocity values.

C. Test of the Markov property

The velocities series in time, $\{v_t^{(n)}\}_{n=1}^\infty$, and space, $\{v_s^{(n)}\}_{n=1}^\infty$, are stochastic processes. In the previous section we observed that the transition probabilities for the temporal process depend strongly on the initial particle velocity, while the spatial process seems to be independent of the initial condition. In the following, we test the Markovianity of both temporal and spatial processes. The transition probabilities for a Markov chain model need to satisfy the Chapman-Kolmogorov equation (e.g., [19]), which reads for the transition matrices $\mathbf{T}(\omega)$ of a discrete Markov chain as

$$\mathbf{T}(\omega + \omega') = \mathbf{T}(\omega)\mathbf{T}(\omega') \quad (24)$$

with $\omega, \omega' > 0$. The latter implies

$$\mathbf{T}(n\omega) = \mathbf{T}^n(\omega). \quad (25)$$

We test the validity of the Chapman-Kolmogorov equation for both temporal and spatial processes numerically by comparing the transition matrix $\mathbf{T}^t(t)^n$ with the transition matrix $\mathbf{T}^t(nt)$, and $\mathbf{T}^s(x)^n$ with the transition matrix $\mathbf{T}^s(nx)$.

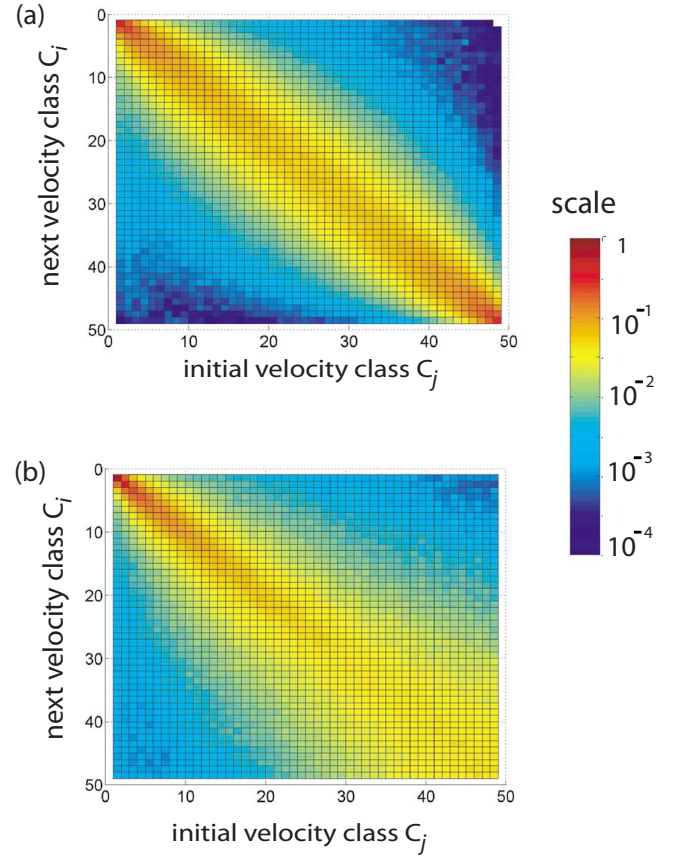


FIG. 7. (Color online) Transition matrix in distance $\mathbf{T}^s(\lambda/2)$ for the multilognormal field and the connected field.

For the transition matrix in time, we find that the Markov property is never confirmed whatever the temporal increment t , see Fig. 8. The expression $\mathbf{T}^t(t)^n$ reproduces well the return probability for high initial velocities but fails for low initial velocities. In addition, the Markov model in time does not predict correctly the probability for particles to make a transition from a low initial velocity to other velocities [Fig. 9(a)] and the probability for particles to make a transition from any velocity to a low velocity zone [Fig. 9(b)].

For the transition matrix in distance, $\mathbf{T}^s(x)$, the Markov property holds for a minimum spatial increment $x = \lambda/2$. It

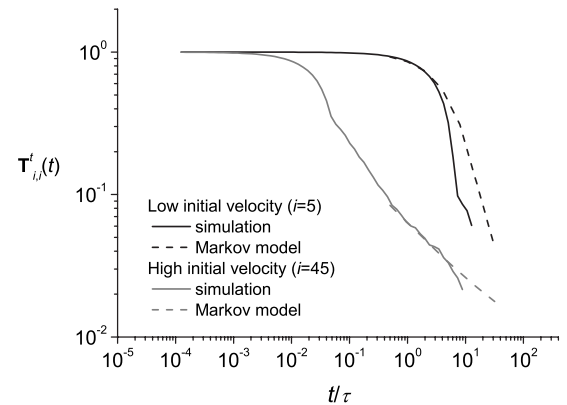


FIG. 8. Comparison of simulation and the Markov model in time for the return probability for the multilognormal field. The Markovian model is defined for a temporal increment $t = \tau/2$.

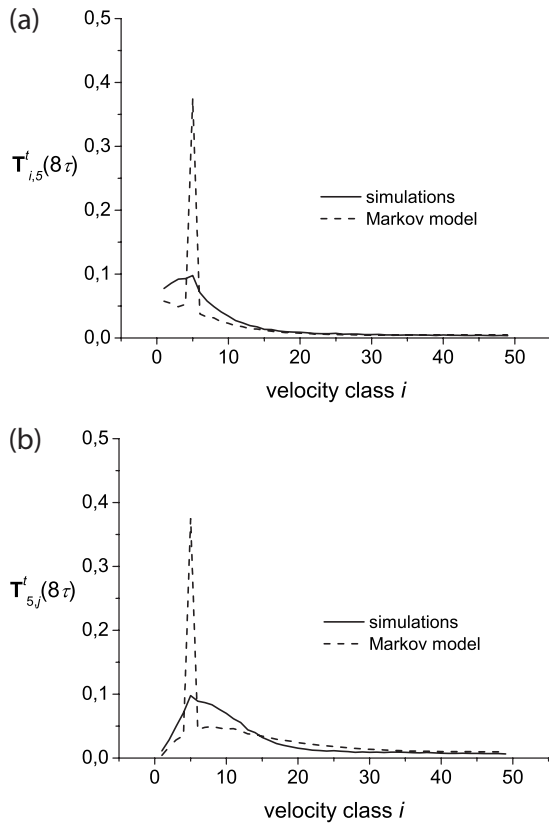


FIG. 9. Comparison of simulation and the Markov model in time for two crosscuts of the velocity transition matrix at time $t = 8\tau$, for the multilognormal hydraulic conductivity field. (a) Velocity class distribution at time $t = 8\tau$ for particles leaving from class C_5 and (b) distribution of velocity class origin for particles arriving at class C_5 at time $t = 8\tau$. As for Fig. 8, the Markov model is defined for a temporal increment $t = \tau/2$.

does not for smaller spatial increments, for which the particle velocities can depend on the previous particle velocities for several steps. This can be attributed to the Gaussian correlation function adopted here [Eq. (7)] for the log permeability field, which imposes a relatively strong correlation at small distances. Figure 10 compares the prediction of the Markov model, i.e., $\mathbf{T}^s(x)^n$ and the result of the simulation for the multilognormal hydraulic conductivity field, i.e., $\mathbf{T}^s(nx)$. The Markov model reproduces well the return probability for the high and low initial velocities (Fig. 10). Contrary to the Markov model in time (Fig. 9), the Markov model in space predicts correctly the transitions from low initial velocities to other velocities [Fig. 11(a)] and the transition from any velocity to a low velocity [Fig. 11(b)].

We performed the same tests for the Markovianity of the velocity transition process for the connected field and found similar results. The Markov model in time fails to reproduce the simulations while the Markov model in space is in good agreement with the simulations. Thus it appears that the spatial Markov model is able to capture the specific velocity correlation properties that characterize the connected field.

The failure of the Markov model in time to represent the velocity transitions is related to the existence of a broad range of characteristic correlation times. The range of char-

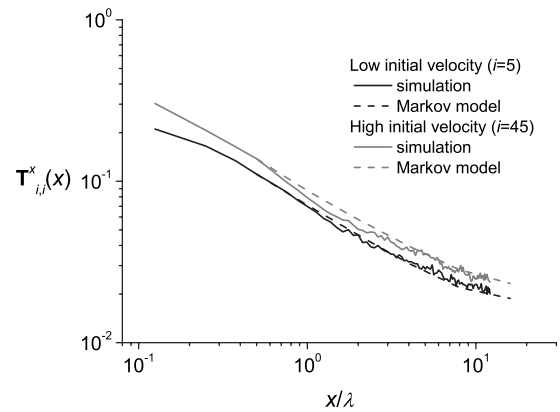


FIG. 10. Comparison of simulation and the Markov model in distance for the return probability for the multilognormal field. The Markov model is defined for a spatial increment $x = \lambda/2$.

acteristic correlation distances is much narrower. The velocity transition process for particles departing from high velocities is well-represented by a Markov model. However, this is not the case for velocity transition for particles with low initial velocities. For these particles, non-Markovian effects occur due to strong velocity correlations.

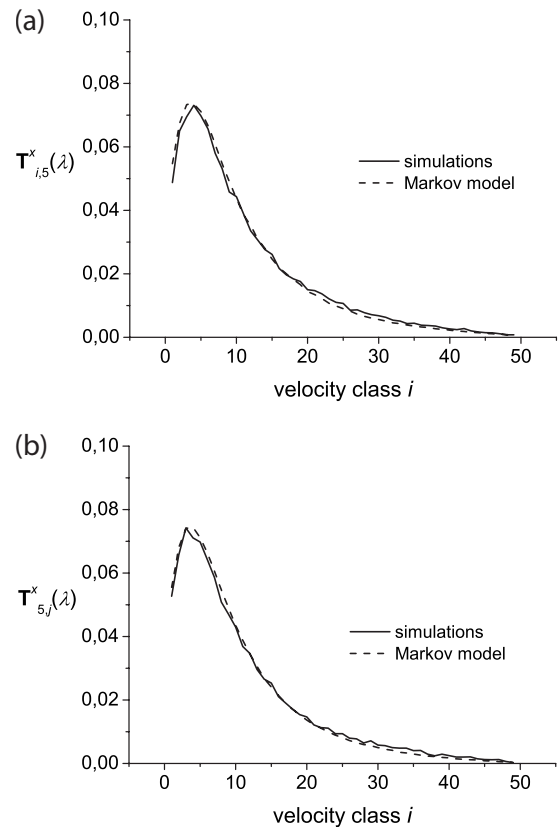


FIG. 11. Comparison of simulation and the Markov model in space for two crosscuts of the velocity transition matrix at distance $x = \lambda$, for the multilognormal hydraulic conductivity field. (a) Velocity class distribution at distance $x = \lambda$ for particles leaving from class C_5 and (b) distribution of velocity class origin for particles arriving at class C_5 at distance $x = \lambda$. As for Fig. 8, the Markov model is defined for a spatial increment $x = \lambda/2$.

Note that we chose a discretization of the Lagrangian velocity field using equiprobable classes because it provides a good way to visualize the Lagrangian velocity transition process and the correlation properties for different organizations of the hydraulic conductivity fields (Figs. 6 and 7). We have tested other discretizations and found similar results.

V. CONCLUSIONS

The analysis of flow and transport in lognormal permeability fields shows that the Lagrangian velocities form a Markov process in space, that is, the Lagrangian velocities taken at equal longitudinal distances along particle trajectories form a Markov process. Thus classical descriptions of particle transport using Markov processes in time [14,26–28], Eq. (16), are not suited for modeling particle movements in such media. This is a direct consequence of the fact that low particle velocities are much more strongly correlated in time than high velocities. The latter is the reason why the effective particle dynamics are non-Markovian in time. This behavior is captured in a systematic way by a Markov model that acknowledges that the Lagrangian velocity is a spatial Markov process. The complex velocity field organization can be quantified by the velocity transition matrix in space (Fig. 7). The latter can be used to characterize and visualize the Lagrangian velocity properties for different velocity field organizations.

The fact that the Lagrangian velocities form a Markov process in space indicates that effective particle movements

can be modeled as a space-time random walk characterized by a constant spatial increment and a random time increment. The sequence of Lagrangian velocities is mapped onto the sequence of temporal displacements by Eq. (17), which then form a Markov process, i.e., an increment at a given step depends on the increment at the previous spatial step. This transport description is consistent with the Lagrangian velocity field correlation properties. Such an effective transport model generalizes the classical CTRW framework to transport in correlated velocity fields. It can be viewed as a persistent CTRW. This effective transport model is developed in [29] and compared to the classical CTRW model. The relevance of the spatial Markov property for different velocity field organizations suggests that such an effective framework may find a wide range of applications for describing transport in heterogeneous flows. We are currently investigating the influence of the Peclet number and the influence of a spatially variable porosity on the Lagrangian velocity correlation properties and on the relevant effective transport model.

ACKNOWLEDGMENTS

Tanguy Le Borgne gratefully acknowledges the financial support of the 6th European Research Framework Program through Marie Curie Intra-European Action Contract No. 023858. Marco Dentz acknowledges the financial support of the Spanish Ministry of Education and Science (MEC) through the program Ramon y Cajal.

-
- [1] G. Dagan, *Flow and Transport in Porous Formations* (Springer, New York, 1989).
 - [2] S. P. Neuman, *Water Resour. Res.* **31**, 1455 (1995).
 - [3] M. Huber, J. C. McWilliams, and M. Ghil, *J. Atmos. Sci.* **58**, 2377 (2001).
 - [4] K. V. Koshel and S. V. Prants, *Phys. Usp.* **49**, 1151 (2006).
 - [5] T. Le Borgne and P. Gouze, *Water Resour. Res.* **44**, W06427 (2008).
 - [6] D. L. Koch and J. F. Brady, *J. Fluid Mech.* **180**, 387 (1987).
 - [7] J. P. Bouchaud and A. Georges, *Phys. Rep.* **195**, 127 (1990).
 - [8] R. Metzler and J. Klafter, *Phys. Rep.* **339**, 1 (2000).
 - [9] H. A. Makse, J. S. Andrade, and H. E. Stanley, *Phys. Rev. E* **61**, 583 (2000).
 - [10] M. Park, N. Kleinfelder, and J. H. Cushman, *Phys. Rev. E* **72**, 056305 (2005).
 - [11] B. Berkowitz, A. Cortis, M. Dentz, and H. Scher, *Rev. Geophys.* **44**, RG2003 (2006).
 - [12] M. Dentz, T. Le Borgne, and J. Carrera, *Phys. Rev. E* **77**, 020101 (2008).
 - [13] T. Le Borgne, J. R. de Dreuzy, P. Davy, and O. Bour, *Water Resour. Res.* **43**, 2006WR004875 (2007).
 - [14] P. S. Berloff and J. C. McWilliams, *J. Phys. Oceanogr.* **32**, 797 (2002).
 - [15] E. W. Montroll and G. H. Weiss, *J. Math. Phys.* **6**, 167 (1965).
 - [16] M. Montero and J. Masoliver, *Phys. Rev. E* **76**, 061115 (2007).
 - [17] M. Dentz and B. Berkowitz, *Phys. Rev. E* **72**, 031110 (2005).
 - [18] J. Bear, *Dynamics of Fluids in Porous Media* (Elsevier, New York, 1972).
 - [19] H. Risken, *The Fokker-Planck Equation* (Springer, Heidelberg, 1996).
 - [20] A. Fiori and G. Dagan, *J. Contam. Hydrol.* **45**, 139 (2000).
 - [21] W. Kinzelbach, *Ground Water Flow and Quality Modelling*, edited by E. Custodio, A. Gurgui, and J. P. Lobo Ferreira (Springer, New York, 1988), pp. 227–246.
 - [22] D. W. Pollock, *Ground Water* **26**, 743750 (1988).
 - [23] B. Zinn and C. F. Harvey, *Water Resour. Res.* **39**, 1051 (2003).
 - [24] C. Knudby and J. Carrera, *J. Hydrol.* **329**, 377 (2006).
 - [25] G. Matheron and G. De Marsily, *Water Resour. Res.* **16**, 901 (1980).
 - [26] G. Pedrizzetti and E. A. Novikov, *J. Fluid Mech.* **280**, 69 (1994).
 - [27] M. Cencini, G. Lacorata, A. Vulpiani, and E. Zambianchi, *J. Phys. Oceanogr.* **29**, 2578 (1999).
 - [28] C. Renner, J. Peinke, and R. Friedrich, *J. Fluid Mech.* **433**, 383 (2001).
 - [29] T. Le Borgne, M. Dentz, and J. Carrera, *Phys. Rev. Lett.* **101**, 090601 (2008).